Journal of the European Ceramic Society 16 (1996) 225–229

0955-2219(95)00155-7
0955-2219/96/$15.00

Mechanical Properties of High Purity Mullite at Elevated Temperatures

H. Ohira,[a] M. G. M. U. Ismail,[a] Y. Yamamoto,[a] T. Akiba[a] & Shigeyuki Sōmiya[b]

[a]Kumagaya Factory, Ceramics Business Div., Chichibu Onoda Cement Corp., 5310 Mikajiri, Kumagaya, Saitama 360, Japan
[b]Faculty of Science and Engineering, The Nishi-Tokyo University, Uenohara, Yamanashi 409-01, Japan

(Accepted 22 July 1995)

Abstract

Microstructures and mechanical properties of stoichiometric mullite (71·8 wt% Al_2O_3/28·2 wt% SiO_2) sintered at different temperatures (1650–1750°C) were studied. Maximum bulk density was obtained by sintering at 1675°C and the density slightly decreased with temperature above 1700°C. Grain size increased with sintering temperature from 1·8 μm at 1650°C to 4·0 μm at 1750°C, and a microstructure comprising a little glassy phase with large elongated grains was observed over 1725°C by scanning electron microscopy. Flexural strength measured below 1500°C decreased with sintering temperature, but creep resistance at 1550°C increased with sintering temperature. Plastic deformation was accompanied by fracture at elevated temperatures.

1 Introduction

High purity mullite is now considered as a prime candidate material for high temperature structural applications because of its excellent high temperature properties. Its flexural strength at room temperature is 300–400 MPa and it is maintained up to 1400°C.[1,2] Excellent creep resistance is also reported.[3–7] But it is reported that the existence of a glassy phase at the grain boundaries has a strong influence on its microstructure and mechanical properties.[8]

As for the stability of mullite at elevated temperature, Prochazka and Klug[9] have suggested that stoichiometric mullite is not stable above a certain temperature. This implies that the microstructure and mechanical properties of stoichiometric mullite will be affected by the sintering temperature.

High purity stoichiometric mullite powder is now produced commercially via the sol–gel process.[10] In the present investigation, the microstructures, flexural strengths and creep resistance of high purity mullite bodies were studied as a function of sintering temperature.

2 Experimental Procedure

Commercial stoichiometric mullite powder (MP40, Chichibu Onoda Cement Corp., Japan) derived via the sol–gel process was used as starting material. Table 1 shows its standard characteristics and Fig. 1 presents a scanning electron micrograph of the as-received MP40. The powder was uniaxially pressed into 50 × 30 × 8 mm blocks and cold isostatically pressed under 200 MPa for 5 min. The blocks were then sintered at 1650, 1675, 1700, 1725 and 1750°C for 2 h in air. Bulk density of the sintered specimens was determined by the liquid displacement method. The sintered bodies were cut into 4 × 3 × 40 mm samples and polished for flexural strength and creep measurements.

Flexural strength and creep resistance were measured by the three-point bending method (Autograph DCS-5000, Shimadzu Corp., Japan) with span of 30 mm. Flexural strength was measured at room temperature, 1400, 1500 and 1600°C with crosshead speed of 0·5 mm min^{-1} in air.

Creep resistance was measured at 1550°C and the strain rate, $\dot{\epsilon}$, and the stress exponent, n, were calculated by following equations:[11]

$$\sigma = \frac{3PL}{2bd^2} \cdot \frac{2n+1}{3n} \quad (1)$$

$$\dot{\epsilon} = \frac{2b(n+2)}{L^2}\dot{y} \quad (2)$$

where σ is the maximum stress, P is the applied load, L is the span length, b is the width of the specimen, d is the thickness of the specimen and $\dot{y}$ is the deflection rate at the load point.

Table 1. Standard characteristics of starting mullite powder (MP40)

Composition (wt%)	Al_2O_3	71·8
	SiO_2	28·2
Impurities (wt%)	TiO_2	<0·1
	Fe_2O_3	<0·01
	Na_2O	<0·01
Average particle size (μm)		1·4
Surface area (BET) ($m^2 g^{-1}$)		8

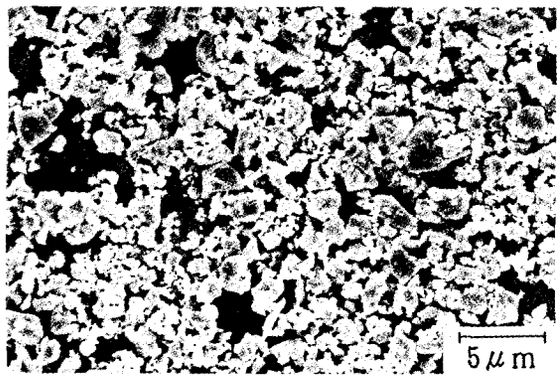

Fig. 1. Scanning electron micrograph of starting mullite powder (MP40).

The microstructure of the specimens was observed by scanning electron microscopy (SEM) (model SIGMA-V, Akashi Seisakusho Co., Ltd., Japan) after polishing and thermal etching. Average grain size was determined by the intercept method.[12]

3 Results and Discussion

3.1 Effects of sintering temperature on density and microstructure

Figure 2 shows the variation of bulk density and average grain size with respect to sintering temperature. Bulk density increased with sintering temperature, reaching a maximum value of 3·14 g cm^{-3} at 1675°C, and then decreased slightly with increase of sintering temperature above 1700°C. The average grain size was 1·8 μm in the 1650°C-sintered specimen and gradually increased with sintering temperature, growing to 4·0 μm at 1750°C.

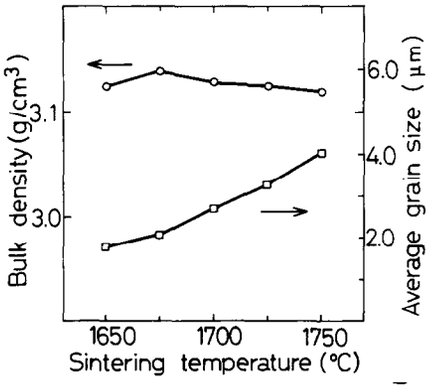

Fig. 2. Variation of bulk density and average grain size of high purity mullite with sintering temperature (duration: 2 h).

Representative microstructures of specimens sintered at different temperatures are shown in Fig 3. In the 1650°C-sintered specimen, many small pores remained, the grains were relatively equiaxial and few elongated grains were observed. However, with the increase of sintering temperature above 1675°C, the grain morphology changed from equiaxial to elongated with the disappearance of the pores. Sintering above 1725°C caused the exaggerated growth of elongated grains, which reached 30 μm in certain cases. Also, small equiaxial grains grew gradually, and a phase separation resulting in the formation of a small amount of glassy phase was observed at the grain boundaries (Fig. 4). The exaggerated grain growth promoted the formation of large pores between the grains and small pores within the grains. The existence of glassy phase at the grain boundaries and the large elongated grain growth suggest that a phase may shift from stoichiometric mullite to high-Al_2O_3 mullite within the solid solution limit and that a liquid phase consisting mainly of SiO_2 may be formed by the phase separation. Prochazka and Klug[9] suggested in their studies on the Al_2O_3–SiO_2 phase diagram that 3:2 mullite is not stable above a certain temperature, and that it forms high alumina mullite with a liquid phase. Thus our present results are consistent with theirs, even though the temperature at which phase separation was observed by SEM in this study was a little higher than the value reported by them.

3.2 Effects of sintering temperature on flexural strength

Figure 5 schematically illustrates load–displacement curves measured at different temperatures for the 1725°C-sintered specimens. The specimen tested at 1400°C showed brittle fracture and little plastic deformation prior to failure. At 1500°C, however, the fracture was brittle but evidence of slight plastic deformation was observed prior to failure. At 1600°C, the specimen fractured with considerable plastic deformation.

Figure 6 shows the variation of flexural strength at room and elevated temperatures as a function of sintering temperature. The data measured at 1600°C were excluded because of significant plastic deformation during the measurements, as shown in Fig. 5. It was evident that the flexural strength decreased with both testing temperature and sintering temperature. As for the relationship between flexural strength and sintering temperature, the strength at room temperature decreased from 400 MPa for the 1675°C-sintered specimen to 300 MPa for the 1750°C-sintered specimen. The

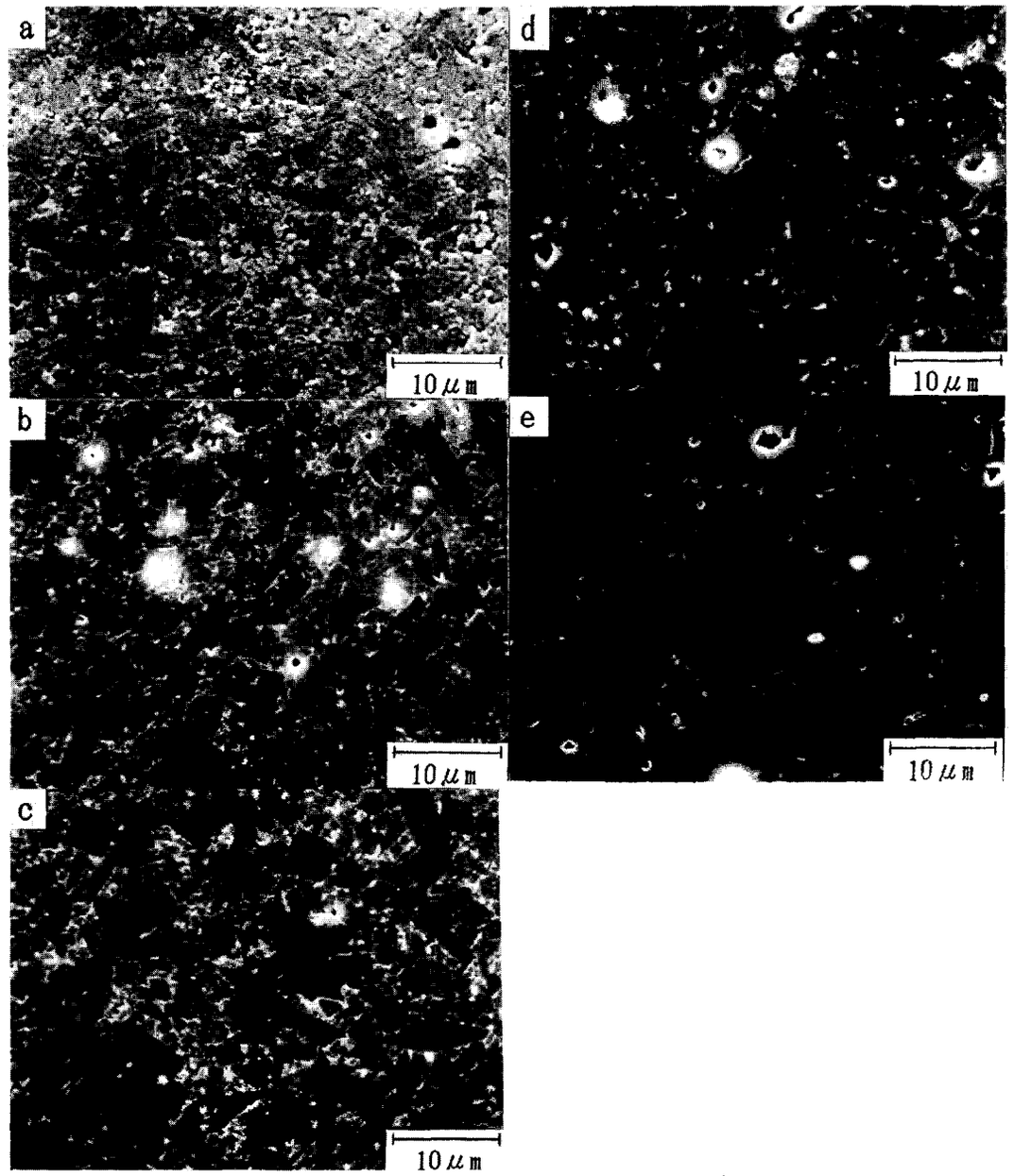

Fig. 3. Scanning electron micrographs of high purity mullite sintered at (a) 1650°C, (b) 1675°C, (c) 1700°C, (d) 1725°C and (e) 1750°C for 2 h (thermally etched at 1550°C).

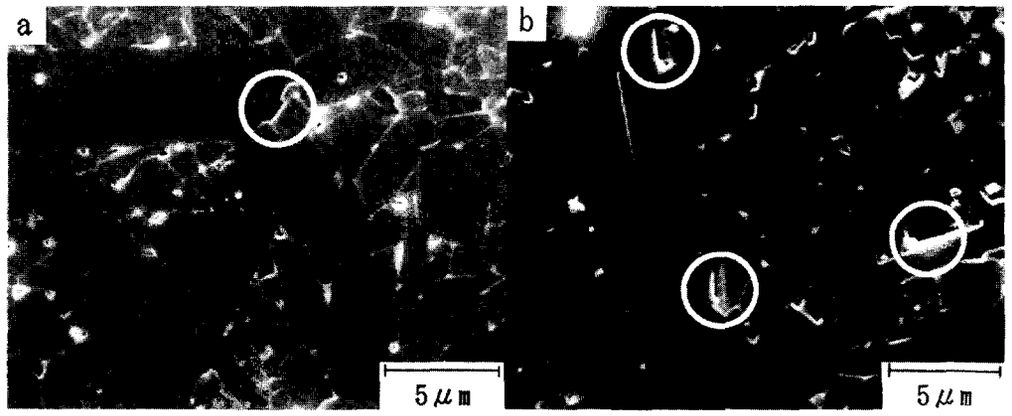

Fig. 4. Scanning electron micrographs of high purity mullite sintered at (a) 1725°C and (b) 1750°C, showing small glassy areas (thermally etched at 1550°C).

strength at 1400°C also decreased from 360 MPa for the 1650°C-sintered specimen to 280 MPa for the 1750°C-sintered specimen. The reason for this strength degradation could be the grain growth, as discussed later. Strength degradation at 1500°C, however, became smaller than those of strength at

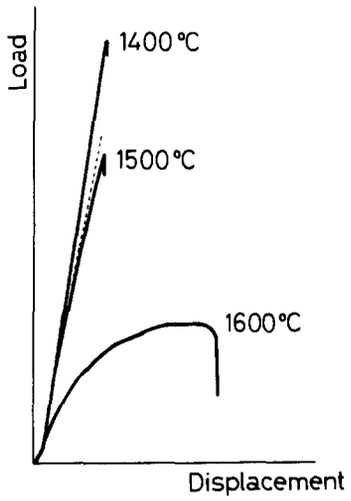

Fig. 5. Schematic illustration of load–displacement curves measured at elevated temperatures for the specimen sintered at 1725°C for 2 h (three-point bending, crosshead speed 0·5 mm min^{-1}).

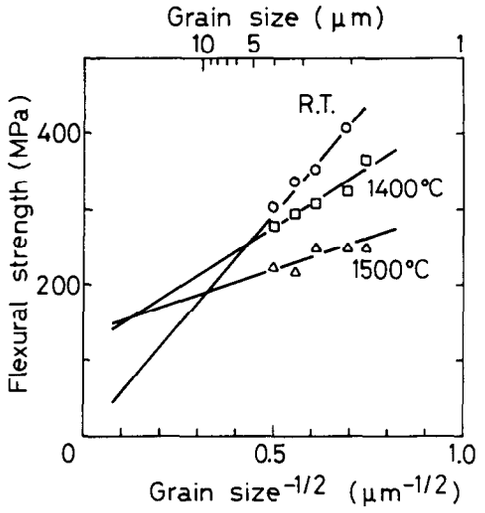

Fig. 7. Variation of flexural strength at different temperatures as a function of average grain size.

room temperature and 1400°C. This observation could be explained by the relation between plastic deformation and the glassy phase. If glassy phase exists at the grain boundaries, plastic deformation at fracture will occur at elevated temperature and the calculated fracture stress will be higher than the real fracture stress. As previously shown in Figs 3 and 4, more glassy phase at grain boundaries was observed at higher sintering temperature. And also, more significant plastic deformation at fracture was observed at higher testing temperature as shown in Fig. 5. Therefore the effects of glassy phase on the fracture stress would be higher for the specimens sintered at higher temperature and, as a result, the strength degradation at 1500°C would become smaller.

Figure 7 shows the relationship between fracture stress and grain size. The relationship followed a Hall–Petch type equation,

$$\sigma_f = \sigma_0 + k\, d^{-1/2} \tag{3}$$

where σ_f is the fracture stress, σ_0 is the stress axis intercept, k is a constant and d is the grain size. Flexural strength at room and elevated temperatures obeyed a Hall–Petch relationship although the intercepts and gradients of the curves differed. The stress-axis intercept of the data at room temperature was close to zero and equation (1) can be expressed as,

$$\sigma_f = k'\, d^{-1/2} \tag{4}$$

where k' is a constant. Equation (4) is equivalent to the Griffith equation by assuming that the critical flaw size is proportional to the grain size, i.e.

$$c = \alpha\, d \tag{5}$$

where c is the critical flaw size and α is a constant. This implies that the specimens would fracture in the brittle manner at room temperature. On the other hand, the fracture stresses measured at 1400 and 1500°C follow Eqn (3) which has been confirmed for a variety of polycrystalline strength phenomena.[13–15] This suggests that fracture at elevated temperatures could be accompanied by plastic flow, although little plastic deformation was observed from the load–displacement curves as shown in Fig. 5. That is, the stress at the crack tip becomes very high at fracture as a result of stress concentration, therefore plastic flow would occur even at 1400°C.

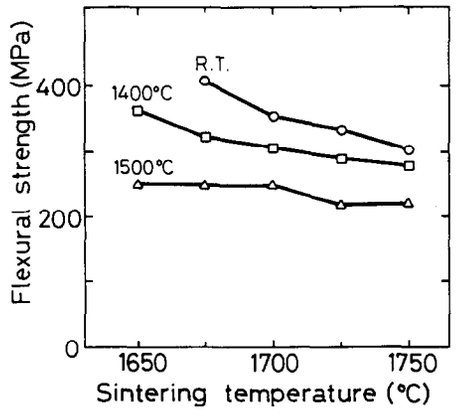

Fig. 6. Variation of flexural strength at different temperatures as a function of sintering temperature.

3.3 Effects of sintering temperature on creep

Figure 8 shows the steady-state creep rate vs. stress from 10 to 100 MPa at 1550°C as a function of sintering temperature. Creep resistance increased with sintering temperature, i.e. with the grain size. The stress exponent, n, of the 1675°C-sintered specimen was 1·3 and that of 1700°C-sintered specimen was 1.2. These similar values suggest that the same creep mechanism was operative in this tem-

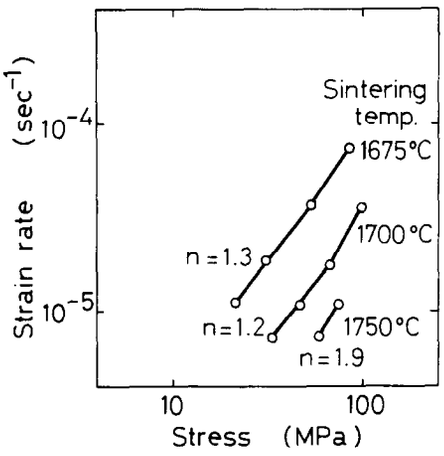

Fig. 8. Steady-state creep rate vs. stress at 1550°C by three-point bending as a function of sintering temperature.

perature region. Some researchers[3,5,6] have reported that the stress exponents of stoichiometric mullite measured by the bending technique are 0·95–1·3 at 1400 and 1500°C, and that the deformation mechanism is diffusional creep. Results of the present study are similar to these reported values, therefore the deformation mechanism for the 1675°C- and 1700°C-sintered specimens of this study may also be diffusional creep although the testing temperature was higher than in previous reports. For the specimen sintered at 1750°C, however, a higher n value of 1·9 was obtained, suggesting that a different creep mechanism was operative. As shown in Fig. 4, the microstructure of this specimen was a little different and a small amount of glassy phase was observed at grain boundaries by SEM observation. Therefore this glassy phase would have influenced the creep behaviour of this specimen.

4 Conclusions

Microstructures and mechanical properties of stoichiometric mullite (71·8 wt% Al_2O_3/28·2 wt% SiO_2) sintered at different temperatures (1650–1750°C) have been studied and following results obtained.

1. Maximum bulk density is obtained by sintering at 1675°C and decreases slightly upon sintering above 1700°C. Grain size increases with sintering temperature from 1·8 μm at 1650°C to 4·0 μm at 1750°C, and a little glassy phase and large elongated grains are observed above 1725°C by SEM.
2. Flexural strength measured below 1500°C decreases with sintering temperature. Plastic deformation is accompanied by fracture even at the temperature of 1400°C, although little plastic deformation prior to failure is observed in load–displacement curves.
3. Creep resistance increases with sintering temperature. The creep mechanism of specimens sintered at 1675 and 1700°C is considered to be diffusional creep, but a different creep mechanism may also be operative for the specimen sintered at 1750°C.

References

1. Kanzaki, S., Tabata, H., Kumazawa, T. & Ohta, S., Sintering and mechanical properties of stoichiometric mullite. *J. Am. Ceram. Soc.*, **68**(1) (1985) C-6–7.
2. Ismail, M. G. M. U., Nakai, Z., Ohira, H. & Sōmiya, S., Preparation and characterization of mullite containing materials. In *Ceramic Powder Science II B*, eds G. R. Messing, E. R. Fuller & H. Hausner, The American Ceramic Society, Inc., Westerville, OH, 1988, pp. 1108–14.
3. Lessing, P. A., Gordon, R. S. & Mazdiyasni, K. S., Creep of polycrystalline mullite. *J. Am. Ceram. Soc.*, **58**(3–4) (1975) 149.
4. Dokko, P. C., Pask, J. A. & Mazdiyasni, K. S., High temperature mechanical properties of mullite under compression. *J. Am. Ceram. Soc.*, **60**(3–4) (1977) 150–5.
5. Ohnishi, H., Maeda, K., Nakamura, T. & Kawanami, T., High temperature mechanical properties of mullite ceramics. In *Mullite and Matrix Composites*, eds S. Sōmiya, R. F. Davis & J. A. Pask, The American Ceramic Society, Inc., Westerville, OH, 1990, pp. 605–12.
6. Okamoto, Y., Fukudome, H., Hayashi, K. & Nishikawa, T., Creep deformation of polycrystalline mullite. *J. Eur. Ceram. Soc.*, **6** (1990) 161–8.
7. Ohira, H., Shiga, H., Ismail, M. G. M. U., Nakai, Z., Akiba, T. & Yasuda, E., Compressive creep of mullite ceramics. *J. Mater. Sci. Lett.*, **10**(14) (1991) 847–9.
8. Kumazawa, T., Kanzaki, S., Ohta, S. & Tabata, H., Influence of chemical composition on the mechanical properties of SiO_2–Al_2O_3 ceramics. *Yogyokyokai-shi*, **96**(1) (1988) 85–91.
9. Prochazka, S. & Klug, F. J., Infrared-transparent mullite ceramic. *J. Am. Ceram. Soc.*, **66**(12) (1986) 874–80.
10. Ismail, M. G. M. U. & Nakai, Z., Properties of high-purity mullite prepared by the sol–gel method. In *Mullite II*, ed. S. Sōmiya, Uchida Rokakuho Publishing Co., Tokyo, Japan, 1987, pp. 69–80.
11. Hollenberg, G. W., Terwillinger, G. R. & Gordon, R. S., Calculation of stresses and strains in four-point bending creep tests. *J. Am. Ceram. Soc.*, **54**(4) (1971) 196–9.
12. Underwood, E. E., *Quantitative Stereology*. Addison-Wesley, 1970.
13. Sinha, M. N., Lloyd, D. J. & Tangri, K., Microyield and fracture in polycrystalline MgO. *J. Mater. Sci.*, **8** (1973) 116–22.
14. Tressler, R. E., Langensiepen, R. A. & Bradt, R. C., Surface-finish effects on strength-vs-grain-size relations in polycrystalline Al_2O_3. *J. Am. Ceram. Soc.*, **57**(5) (1974) 226–7.
15. Bradt, R. C., Dulberg, J. L. & Tressler, R. E., Surface finish effects and the strength-grain size relationship in MgO. *Acta Metall.*, **24** (1976) 529–34.